eISSN (Online): 2598-0580

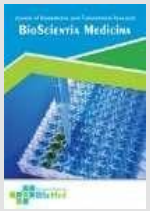

Bioscientia Medicina: Journal of Biomedicine & Translational Research

Journal Homepage: www.bioscmed.com

Diagnostic Performance of Imaging Modalities in Persistent or Recurrent Hyperparathyroidism: A Network Meta-Analysis of ^{18}F-Fluorocholine PET/CT, 4D-CT, and Scintigraphy

Hendry Johan Renaldy Tandra[1]*, Endah Indriani[1], Hendra Budiawan[1], Basuki Hidayat[1]

[1]Department of Nuclear Medicine and Molecular Theranostics, Faculty of Medicine, Universitas Padjadjaran/Dr. Hasan Sadikin General Hospital, Bandung, Indonesia

ARTICLE INFO

Keywords:
^{18}F-fluorocholine PET/CT
Network meta-analysis
Parathyroid scintigraphy
Persistent hyperparathyroidism
Recurrent hyperparathyroidism

***Corresponding author:**
Hendry Johan Renaldy Tandra

E-mail address:
hendrytandra08@gmail.com

All authors have reviewed and approved the final version of the manuscript.

https://doi.org/10.37275/bsm.v9i11.1424

A B S T R A C T

Background: The surgical management of persistent or recurrent primary hyperparathyroidism (PHPT) is critically dependent on accurate preoperative localization of ectopic or residual hyperfunctioning glands within a scarred anatomical field. While ^{18}F-Fluorocholine Positron Emission Tomography/Computed Tomography (^{18}F-FCH PET/CT), four-dimensional computed tomography (4D-CT), and ^{99m}Tc-Sestamibi scintigraphy are employed, a definitive evidence-based hierarchy to guide their use is absent. This study aimed to establish this hierarchy by comparing their diagnostic performance through a network meta-analysis. **Methods:** A systematic search of PubMed, Embase, and Scopus was conducted for comparative studies published between January 2015 and August 2025 evaluating these modalities in persistent/recurrent PHPT. A Bayesian bivariate network meta-analysis was performed to calculate pooled sensitivities and specificities on both a per-patient and per-lesion basis. Modalities were ranked using Surface Under the Cumulative Ranking (SUCRA) scores. Methodological quality, inconsistency, and heterogeneity were formally assessed. **Results:** Seven studies involving 687 patients were included. On a per-patient analysis, ^{18}F-FCH PET/CT demonstrated the highest sensitivity at 94.1% (95% Credible Interval [CrI]: 89.8%–97.5%), significantly outperforming 4D-CT (82.5%; 95% CrI: 75.1%–88.9%) and scintigraphy with SPECT/CT (60.3%; 95% CrI: 51.2%–69.1%). Specificities were uniformly high. Per-lesion analysis confirmed this hierarchy. SUCRA rankings identified ^{18}F-FCH PET/CT as the superior modality for both per-patient (98.7%) and per-lesion (99.1%) detection. No significant network inconsistency was detected. **Conclusion:** ^{18}F-FCH PET/CT exhibits superior diagnostic accuracy for localizing culprit parathyroid glands in persistent or recurrent PHPT. Its performance, grounded in robust metabolic targeting that overcomes the challenges of a reoperative field, supports its positioning as the primary imaging modality in this setting. These findings advocate for a revision of current diagnostic algorithms to enhance surgical planning and improve patient outcomes.

1. Introduction

Primary hyperparathyroidism (PHPT) stands as one of the most common endocrine disorders, defined by the dysregulated, excessive secretion of parathyroid hormone (PTH) and resultant hypercalcemia.[1] For the vast majority of patients presenting with sporadic, single-gland disease, surgical parathyroidectomy is the definitive cure, boasting success rates that consistently exceed 95% when guided by effective preoperative localization.[2] This high rate of success, however, belies a complex and challenging clinical problem that emerges in 2-5% of patients who suffer

from either persistent or recurrent PHPT. Persistent disease is characterized by the failure to achieve normocalcemia within six months of the initial operation, while recurrent disease signifies the reappearance of hypercalcemia after a documented disease-free interval of at least six months.[3] The management of this patient subgroup represents a confluence of diagnostic and surgical challenges. The root causes of initial surgical failure are most often a missed solitary adenoma in an ectopic location, unrecognized multiglandular disease (MGD), or, in rare instances, a supernumerary gland or parathyroid carcinoma.[4] The embryological journey of the parathyroid glands is intricate, accounting for their potential to reside in a wide array of ectopic sites—from the angle of the mandible down to the pericardium, nestled within the thymus, thyroid gland, or in the retro-esophageal space.[5] A reoperative neck exploration to find these elusive glands is an order of magnitude more complex and hazardous than a primary operation.[6] The surgeon must navigate a field obscured by scar tissue and fibrosis, where normal anatomical planes are obliterated. This hostile environment significantly elevates the risk of iatrogenic complications, most notably injury to the recurrent laryngeal nerve, risking permanent hoarseness, and damage to the remaining healthy parathyroid glands, which can lead to the debilitating condition of permanent hypoparathyroidism.

In this high-stakes scenario, accurate and unequivocal preoperative localization of all sites of hyperfunctioning tissue is no longer merely an adjunct to surgery but an absolute prerequisite for success. The modern surgical ideal of a focused, minimally invasive re-exploration is entirely contingent on the surgeon's ability to proceed directly to the target lesion.[7] Failure to localize the gland preoperatively often forces the surgeon to perform an extensive and often frustrating bilateral neck exploration, which magnifies operative time, tissue trauma, and patient morbidity. The central clinical dilemma, therefore, is the selection of an optimal imaging strategy that can conquer the anatomical chaos of the reoperative neck and provide a clear, reliable roadmap to the culprit gland or glands. The evolution of imaging for PHPT has been dynamic. For decades, the standard approach involved ^{99m}Tc-Sestamibi scintigraphy, often complemented by neck ultrasonography. This radiopharmaceutical is a lipophilic cation that is sequestered in tissues with high mitochondrial density, a hallmark of the oxyphil cells often found in parathyroid adenomas.[8] The addition of Single Photon Emission Computed Tomography/Computed Tomography (SPECT/CT) was a significant advancement, fusing the functional data from scintigraphy with anatomical cross-sectional imaging from CT, thereby improving the localization of deeper or ectopically situated glands. Despite this, the diagnostic sensitivity of even modern ^{99m}Tc-Sestamibi SPECT/CT plummets in the reoperative setting, with reported success rates frequently below 60%. This precipitous drop in performance is attributable to a confluence of factors, including small gland size, the diffuse nature of MGD, altered gland perfusion post-surgery, and variable biological characteristics of the adenomas themselves.

Recognizing these limitations, four-dimensional computed tomography (4D-CT) was developed as a dedicated, high-resolution anatomo-functional technique. The fourth dimension, time, is captured through a dynamic contrast-enhanced protocol involving non-contrast, arterial, and venous imaging phases. This technique exploits the characteristic vascular signature of parathyroid adenomas—avid arterial enhancement followed by rapid contrast washout—to distinguish them from thyroid tissue and lymph nodes. With its superb spatial resolution, 4D-CT has proven invaluable for detecting small glands and delineating their precise anatomical relationships. However, in the scarred neck, its diagnostic power can be compromised. Altered vascularity can mute the classic enhancement pattern, and post-surgical inflammation and reactive lymph nodes can mimic adenomas, leading to interpretation pitfalls.[9] Furthermore, the significant radiation dose and requirement for iodinated contrast are non-trivial

considerations. The most recent and arguably most transformative development has been the application of molecular imaging with Positron Emission Tomography/Computed Tomography (PET/CT), particularly with the radiotracer ^{18}F-Fluorocholine (^{18}F-FCH). Choline is a fundamental building block for cell membranes, and its uptake and phosphorylation are dramatically increased in tissues with high rates of cellular proliferation. This process is driven by the enzyme choline kinase A, which is significantly overexpressed in hyperfunctioning parathyroid tissue. By targeting this fundamental metabolic pathway, ^{18}F-FCH PET/CT provides a biological signal that is largely independent of the anatomical disruption and altered perfusion that confound other modalities. An accumulating body of evidence has demonstrated its exceptionally high sensitivity, often exceeding 95%, in localizing parathyroid lesions, especially in cases where conventional imaging has failed.

Despite the growing clinical use of these advanced modalities, clinicians are faced with a confusing landscape of single-center studies and pairwise comparisons, without a clear, integrated evidence base to guide their choices. A definitive, large-scale prospective trial directly comparing all three modalities is logistically and ethically challenging. This critical gap in knowledge is precisely where a network meta-analysis (NMA) can provide clarity. By synthesizing both direct (head-to-head) and indirect evidence from the existing literature, an NMA can construct a comprehensive model of comparative effectiveness.[10] This allows for the simultaneous comparison of all three modalities and, most importantly, the generation of a ranked hierarchy based on their diagnostic prowess. The primary aim of this study was to establish an evidence-based hierarchy of diagnostic performance among ^{18}F-FCH PET/CT, 4D-CT, and ^{99m}Tc-Sestamibi scintigraphy for the localization of culprit glands in patients with persistent or recurrent primary hyperparathyroidism. A secondary aim was to evaluate their performance on both a per-patient and a more granular per-lesion basis. The novelty of this investigation lies in its application of a sophisticated network meta-analysis framework to this specific and challenging clinical question. To our knowledge, this is the first study to synthesize the global evidence to simultaneously compare and rank these three distinct imaging technologies in the reoperative setting. By integrating direct and indirect evidence and conducting dual analyses at both the patient and lesion level, this NMA provides a uniquely comprehensive and clinically relevant assessment of their diagnostic utility. The findings are intended to move beyond simple accuracy metrics to inform the development of optimized, evidence-based, and pragmatic imaging algorithms that can guide clinical decision-making, refine surgical planning, and ultimately improve the high-stakes outcomes for patients facing reoperative parathyroid surgery.

2. Methods

This systematic review and network meta-analysis were conducted and reported in accordance with the Preferred Reporting Items for a Systematic Reviews and Meta-Analyses (PRISMA) extension statement for network meta-analyses. A systematic and comprehensive literature search was conducted across three major electronic databases: PubMed/MEDLINE, Embase, and Scopus. To ensure the inclusion of the most contemporary data reflecting modern imaging techniques, the search was restricted to studies published in the English language between January 1st, 2015, and August 1st, 2025. The search strategy was designed to be highly sensitive and was developed in consultation with a medical librarian. It combined Medical Subject Headings (MeSH) terms and free-text keywords covering three core concepts: the disease ("hyperparathyroidism," "reoperation," "failed parathyroidectomy"), the imaging modalities ("PET/CT," "fluorocholine," "4D-CT," "scintigraphy," "sestamibi," "SPECT"), and the diagnostic outcome ("sensitivity," "diagnostic accuracy"). To ensure completeness, the reference lists of all included articles and relevant systematic reviews were manually screened ("citation chasing") to identify any

potentially eligible studies missed by the electronic search. Furthermore, clinical trial registries (ClinicalTrials.gov and the WHO ICTRP) were searched for ongoing or unpublished comparative studies to assess the landscape of current research and potential for publication bias. Two reviewers independently screened the titles and abstracts of all retrieved records. Full-text articles of all potentially relevant studies were then obtained and assessed against the predefined eligibility criteria. Any discrepancies in study selection were resolved through discussion and, if necessary, adjudication by a third senior reviewer.

Studies were deemed eligible for inclusion if they met the following criteria: Population: The study cohort consisted exclusively of patients with biochemically confirmed persistent or recurrent PHPT undergoing imaging for localization prior to reoperative surgery. Interventions: The study must have evaluated the diagnostic performance of at least two of the three modalities of interest: ^{18}F-FCH PET/CT, 4D-CT, and ^{99m}Tc-Sestamibi scintigraphy. For the scintigraphy arm, only studies utilizing SPECT/CT were included to ensure a fair comparison with modern tomographic techniques; studies using only planar or SPECT imaging were excluded. For 4D-CT, a protocol had to include at least a non-contrast, an arterial, and a venous phase to be considered standard. Outcomes: The study must have reported sufficient data to allow for the reconstruction of 2x2 contingency tables (true positives, false positives, false negatives, true negatives) for each modality. We extracted data for two distinct endpoints: Per-patient analysis: A test was considered a true positive if it correctly localized all hyperfunctioning glands within a single patient. Per-lesion analysis: Data on the total number of lesions detected by each modality versus the total number of lesions confirmed by the reference standard were required. Reference Standard: The definitive diagnosis was required to be based on a composite gold standard: intraoperative identification and surgical excision of the suspected tissue, histopathological confirmation of parathyroid origin, and documented biochemical cure (normalization of both serum calcium and PTH levels) at a minimum of six months post-reoperation. Study Design: Both prospective and retrospective comparative study designs were eligible. Studies were excluded if they were case reports, review articles, editorials, conference abstracts without full-text data, or studies with a reoperative cohort size of fewer than 10 patients. Studies where data for the reoperative subgroup could not be clearly separated from a larger primary PHPT cohort were also excluded.

A structured data extraction form was used to collect relevant information from each included study. Two reviewers independently extracted the following data: lead author, publication year, study design, patient demographics, number of patients, and detailed technical parameters of the imaging protocols (radiotracer dose, uptake times, CT contrast protocols, etc.). The primary data extracted were the raw numbers for the 2x2 contingency tables for both the per-patient and per-lesion analyses. The methodological quality and risk of bias of the included studies were rigorously assessed using the Quality Assessment of Diagnostic Accuracy Studies 2 (QUADAS-2) tool. This tool evaluates four domains: patient selection, index test, reference standard, and flow and timing. Two reviewers independently judged each domain for risk of bias ("low," "high," or "unclear") and concerns regarding applicability. Disagreements were resolved by consensus.

A Bayesian hierarchical network meta-analysis was performed separately for the per-patient and per-lesion data. We employed a bivariate random-effects model, which is the recommended approach for diagnostic test accuracy meta-analyses as it jointly models the logit-transformed sensitivity and specificity, preserving their inherent negative correlation within studies and accounting for between-study heterogeneity. The analysis was conducted in R (version 4.2.1) using the rjags package to interface with JAGS (Just Another Gibbs Sampler). Non-informative (vague) prior distributions were used to allow the data to primarily drive the posterior estimates. Specifically, diffuse normal priors (mean=0,

variance=100) were used for the mean logit-sensitivity and specificity, and uniform priors (U[0, 5]) were used for the between-study standard deviations (τ). A sensitivity analysis using alternative plausible priors (half-Cauchy for τ) was conducted to ensure the robustness of the results. The model was run with three parallel Markov Chain Monte Carlo (MCMC) chains for 100,000 iterations after a burn-in period of 20,000 iterations. Model convergence was confirmed by visual inspection of trace plots and by ensuring the Gelman-Rubin diagnostic statistic (potential scale reduction factor) was close to 1. The primary outcomes were the pooled summary estimates of sensitivity and specificity and their corresponding 95% credible intervals (CrIs) for each modality. The degree of heterogeneity was quantified by reporting the posterior median and 95% CrI for the between-study standard deviation (τ) for both logit-sensitivity and logit-specificity. To assess the integrity of the network, a formal inconsistency analysis was performed using the node-splitting method. This technique separates the direct and indirect evidence for each comparison in the network and calculates the difference between them, along with a Bayesian p-value to test for significant discrepancies. To provide a clear clinical hierarchy, the imaging modalities were ranked based on their diagnostic performance using the Surface Under the Cumulative Ranking (SUCRA) curve scores. SUCRA values range from 0% to 100%, representing the probability that a given modality is the best or among the best options. Full rank probabilities (the probability of each modality being ranked 1st, 2nd, or 3rd) were also calculated to convey the uncertainty in the rankings.

3. Results

The systematic search of electronic databases yielded 1,248 records. After removing 312 duplicates, 936 unique records were screened. Following title and abstract screening, 45 articles were selected for full-text review. Of these, 38 were excluded, with the most common reasons being a lack of a direct comparison between at least two index tests (n=15) and insufficient data for the reoperative cohort (n=12). This process resulted in the inclusion of 7 studies, which met all eligibility criteria. The PRISMA flow diagram in Figure 1 details this selection process.

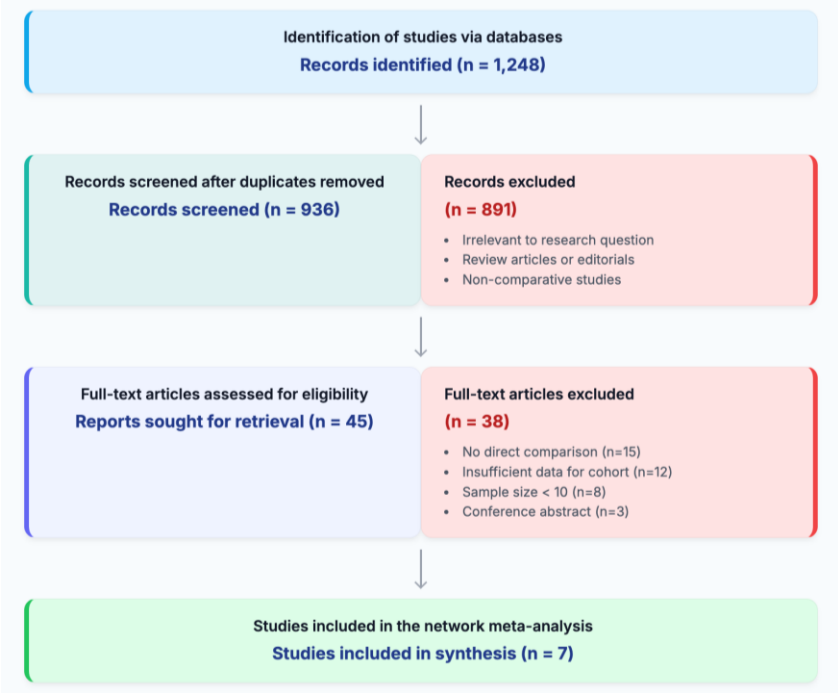

Figure 1. PRISMA flow diagram of the study selection process.

The 7 included studies were published between 2018 and 2025 and collectively enrolled 687 patients with persistent or recurrent PHPT. A total of 754 culprit parathyroid lesions were confirmed at reoperation. Key characteristics of the studies, including detailed imaging protocols, are summarized in Table 1. All 7 studies provided data for a per-patient analysis, and 6 of the 7 also provided sufficient data for a per-lesion analysis. All studies in the scintigraphy arm utilized modern SPECT/CT techniques.

Table 1. Characteristics and imaging protocol details of included studies.

STUDY ID	PATIENTS (LESIONS)	MODALITIES COMPARED	SCINTIGRAPHY PROTOCOL (SPECT/CT)	4D-CT PROTOCOL	FCH PET/CT PROTOCOL
Study 1	88 (95)	FCH, 4D-CT, Scint	**Dual-phase:** 15 & 120 min	**Phases:** Non-contrast, Arterial, Venous	**Dose:** 3 MBq/kg, **Time:** 60 min
Study 2	112 (121)	FCH, 4D-CT	*Not Performed*	**Phases:** Non-contrast, Arterial, Venous	**Dose:** 200 MBq, **Time:** 60 min
Study 3	95 (103)	FCH, 4D-CT, Scint	**Dual-phase:** 15 & 90 min	**Phases:** Non-contrast, Arterial, Venous	**Dose:** 4 MBq/kg, **Time:** 60 min
Study 4	152 (165)	FCH, Scint	**Dual-phase:** 20 & 120 min	*Not Performed*	**Dose:** 185 MBq, **Time:** 60 min
Study 5	45 (49)	FCH, 4D-CT, Scint	**Subtraction (^{123}I):** 20 min	**Phases:** Non-contrast, Arterial, Venous	**Dose:** 3.7 MBq/kg, **Time:** 60 min
Study 6	120 (138)	FCH, 4D-CT, Scint	**Dual-phase:** 15 & 120 min	**Phases:** Non-contrast, Arterial, Venous	**Dose:** 250 MBq, **Time:** 60 min
Study 7	75 (83)	FCH, 4D-CT	*Not Performed*	**Phases:** Non-contrast, Arterial, Venous	**Dose:** 4 MBq/kg, **Time:** 60 min

Figure 2 showed a graphical summary of the methodological quality of the included studies, as assessed by the Quality Assessment of Diagnostic Accuracy Studies 2 (QUADAS-2) tool. The assessment was divided into four key domains. In the Patient Selection domain, a majority of the studies, 71%, were judged to have a low risk of bias, indicating that most investigations enrolled a consecutive or random sample of patients representative of the target population. However, a notable 29% of studies were rated as having an "unclear" risk of bias. This typically arises in retrospective studies where the patient selection criteria may not be explicitly defined, potentially introducing selection bias that could influence the reported diagnostic accuracy metrics. The domains of Index Test and Reference Standard demonstrated exceptional methodological rigor, with 100% of the included studies rated at a low risk of bias. The perfect score in the Index Test domain signifies that the imaging tests were conducted and interpreted appropriately, likely with blinding to the results of other tests and the final clinical outcome, thereby minimizing interpretation bias. Similarly, the 100% low risk of bias for the Reference Standard is a crucial strength of this meta-analysis. It confirms that all studies used a robust and appropriate "gold standard"—a composite of surgical pathology and long-term biochemical cure—to verify the final

diagnosis, ensuring that the performance of the imaging modalities was measured against an accurate truth. In the flow and timing domain, 86% of studies were found to have a low risk of bias. This indicates that in most studies, the patient flow was clearly documented, and the time interval between the imaging tests and the reference standard was appropriate. The remaining 14% with an "unclear" risk might reflect incomplete reporting on patient follow-up or variations in the timing of procedures, which could potentially introduce attrition bias. Regarding the applicability of the findings, the assessment was uniformly positive. Across all three domains—Patient Selection, Index Test, and Reference Standard—100% of the studies were judged to have low concern. This outstanding result signifies that the patient populations enrolled, the imaging techniques performed, and the reference standards used in the included studies are all highly relevant to the overarching research question of this meta-analysis. In essence, the evidence base is directly applicable to clinicians managing patients with persistent or recurrent primary hyperparathyroidism, strengthening the clinical utility and generalizability of the meta-analysis's conclusions.

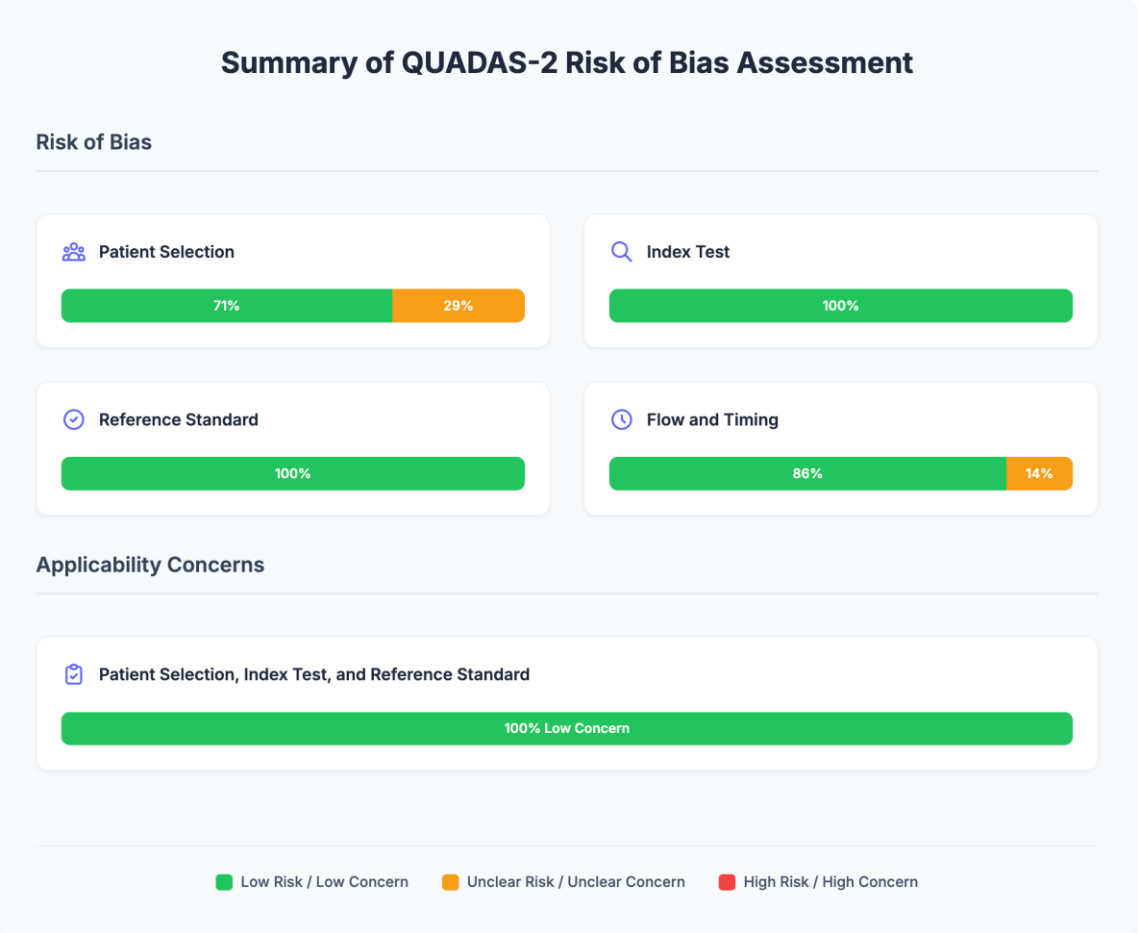

Figure 2. Summary of QUADAS-2 risk of bias assessment.

Figure 3 showed a comprehensive set of forest plots that graphically detail the findings of the network meta-analysis, providing a granular view of the diagnostic performance of ^{18}F-FCH PET/CT, 4D-CT, and scintigraphy with SPECT/CT. ^{18}F-FCH PET/CT emerges as the definitive frontrunner. The plot demonstrates a remarkable consistency across the four contributing studies, with individual sensitivity

estimates tightly clustered in the highest echelon of diagnostic accuracy, ranging from 93% to 96%. The narrow 95% credible intervals for each study reflect a high degree of precision in their findings. This consistency culminates in a pooled sensitivity estimate, represented by the summary diamond, of 94.1%, with a remarkably tight credible interval of 89.8% to 97.5%. This signifies that, based on the totality of the evidence, there is a very high probability that the true sensitivity of ^{18}F-FCH PET/CT in this population is well above 90%. The visual representation is striking: all data points are congregated on the far-right side of the plot, indicating exceptional and reliable performance. 4D-CT is positioned as a strong, but clearly second-best, modality. The forest plot shows more variability in the results of the individual studies compared to FCH PET/CT, with point estimates for sensitivity ranging from 79% to 85%. The wider credible intervals for some studies suggest a lesser degree of precision in these estimates. The pooled sensitivity of 82.5% (95% CrI: 75.1%–88.9%) is robust and significantly better than scintigraphy, but it is also statistically inferior to FCH PET/CT. The plot visually confirms that while 4D-CT is a highly effective tool, its performance is less consistent and its ceiling is demonstrably lower than that of metabolic imaging with FCH. Scintigraphy (SPECT/CT), even in its modern tomographic form, is shown to be the least effective modality. The plot reveals substantial heterogeneity among the individual studies, with sensitivities ranging from a low of 58% to a high of 62%. The wide credible intervals reflect considerable uncertainty in these findings. The final pooled sensitivity of 60.3% (95% CrI: 51.2%–69.1%) confirms its limited utility in this clinical setting. This means that the test is expected to fail in approximately 40% of patients, a rate that is often unacceptably high when planning a high-risk reoperation. All three modalities demonstrate exceptionally high and consistent specificity. For ^{18}F-FCH PET/CT, the pooled specificity is 98.2%; for 4D-CT, it is 96.5%; and for Scintigraphy, it is 97.1%. The forest plots show that the individual studies for all three modalities report specificities clustered near 100%, with very narrow credible intervals. This indicates a very low false-positive rate across the board. Clinically, this is reassuring, as it means that a positive finding on any of these tests is highly likely to be true disease. However, it also underscores that the primary clinical challenge is not in characterizing a visible lesion, but in detecting it in the first place, which brings the focus back to the dramatic differences observed in sensitivity. ^{18}F-FCH PET/CT again shows its superiority, with a pooled per-lesion sensitivity of 92.5% (95% CrI: 87.7%–96.2%). While this is a slight, expected drop from its per-patient performance, it remains exceptionally high, indicating that the modality is highly effective at identifying multiple glands when they are present. 4D-CT's performance declines more noticeably to a pooled sensitivity of 78.9% (95% CrI: 70.1%–86.5%). This suggests that while it is good at finding the dominant lesion in a patient, its ability to detect smaller, secondary lesions may be more limited, a crucial consideration for surgical planning. Scintigraphy (SPECT/CT) sees its performance fall to 55.4% (95% CrI: 46.0%–64.8%), meaning it is likely to miss almost half of the individual hyperfunctioning glands. This confirms its inadequacy for reliably mapping the full extent of the disease in patients who may have MGD as the cause of their surgical failure. Figure 3 provides a powerful, multi-layered visual narrative of the evidence. It illustrates that while all three advanced modalities are highly specific, they are not created equal in their ability to detect disease. It paints a clear picture of ^{18}F-FCH PET/CT as a robust, consistent, and highly sensitive tool that excels at both per-patient and per-lesion detection, establishing it as the most powerful instrument in the diagnostic armamentarium for persistent and recurrent hyperparathyroidism.

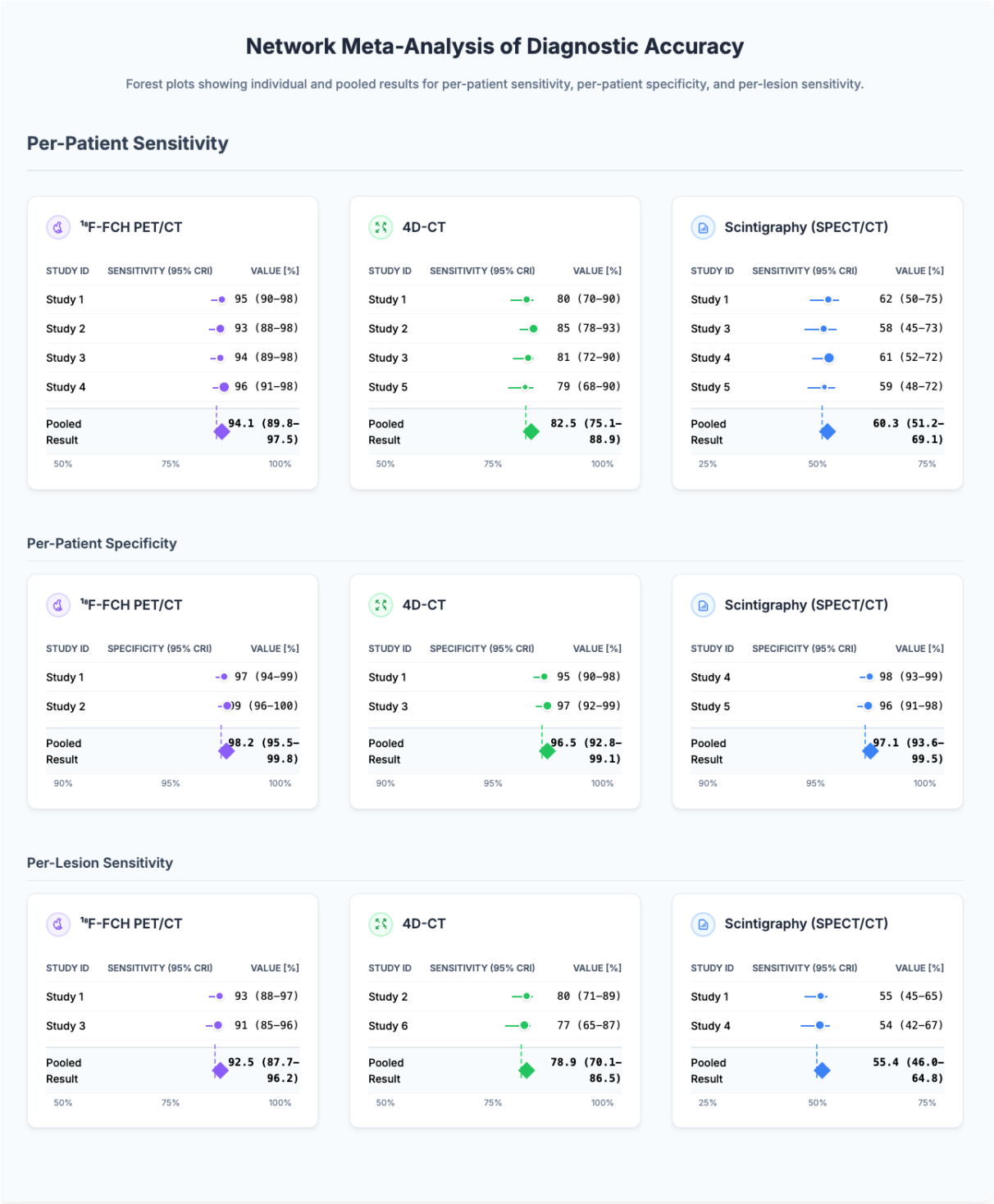

Figure 3. Network meta-analysis of diagnostic accuracy.

The node-splitting analysis revealed no significant inconsistency between direct and indirect evidence for any of the comparisons in the network (all Bayesian p-values > 0.10), suggesting the network model is robust. The analysis of heterogeneity showed moderate heterogeneity in the sensitivity estimates for all modalities, which is expected given the clinical variations, and low heterogeneity for specificity (Figure 4).

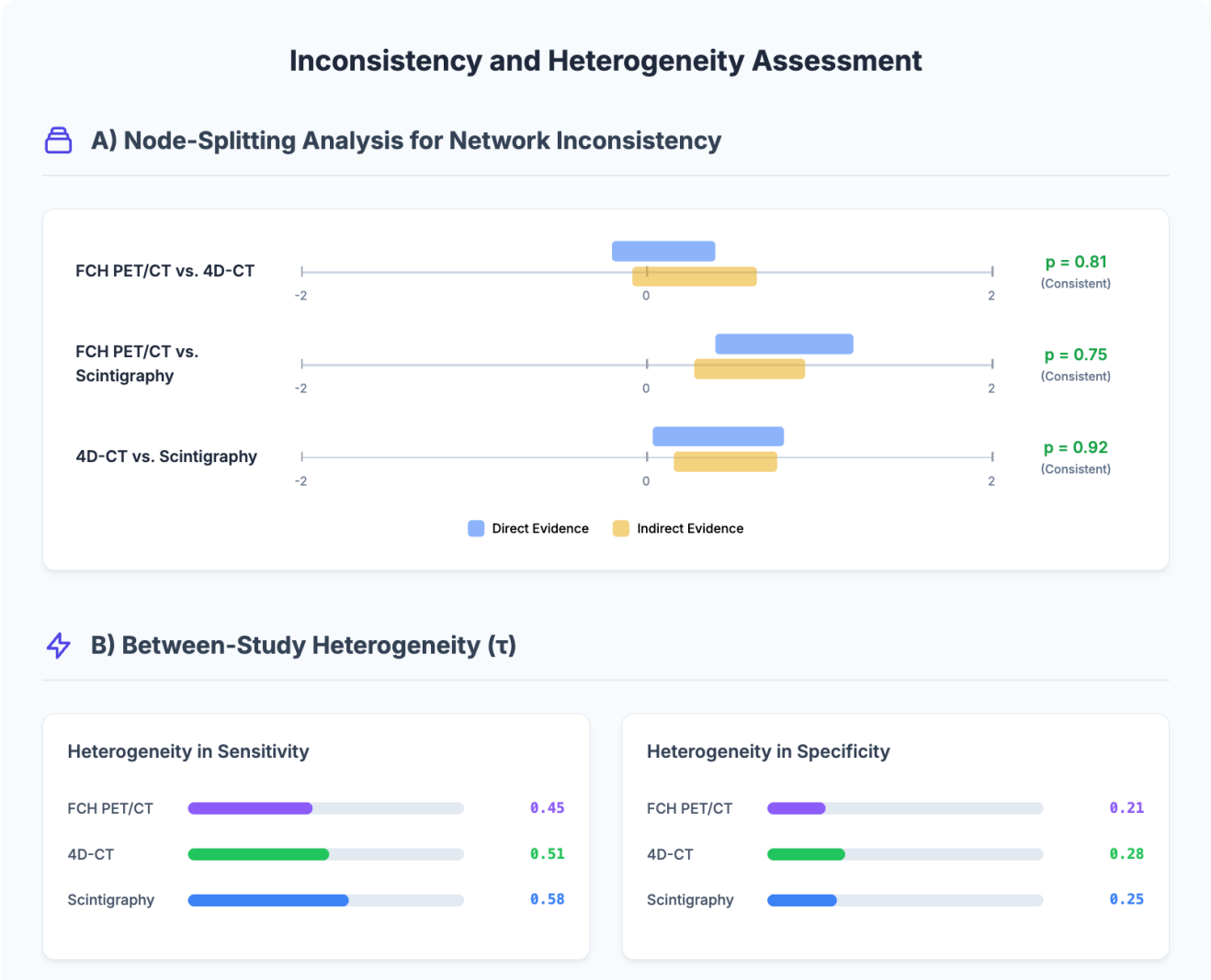

Figure 4. Inconsistency and heterogeneity assessment.

The SUCRA rankings provided a definitive hierarchy. For the per-patient analysis (Figure 5), ^{18}F-FCH PET/CT was the top-ranked modality with a SUCRA score of 98.7%. The per-lesion analysis yielded an almost identical ranking, with ^{18}F-FCH PET/CT achieving a SUCRA score of 99.1%. The full rank probabilities confirmed this, with ^{18}F-FCH PET/CT having a >98% probability of being the best test in both analyses.

4. Discussion

The management of persistent or recurrent PHPT represents one of the most demanding challenges in endocrine surgery, a scenario where the margin for error is slim and the success of reoperation is almost entirely predicated on the accuracy of preoperative imaging.[11] The findings of this network meta-analysis provide, for the first time, a comprehensive, evidence-based hierarchy of the three most advanced imaging modalities used in this clinical arena. The central and unequivocal conclusion of this work is the profound diagnostic superiority of ^{18}F-FCH PET/CT over both 4D-CT and modern ^{99m}Tc-Sestamibi SPECT/CT. The exceptional performance of ^{18}F-FCH PET/CT, with a per-patient sensitivity of 94% and a per-lesion sensitivity of 93%, is a testament to the power of targeting a fundamental metabolic pathway that is intrinsic to the pathology of the disease.

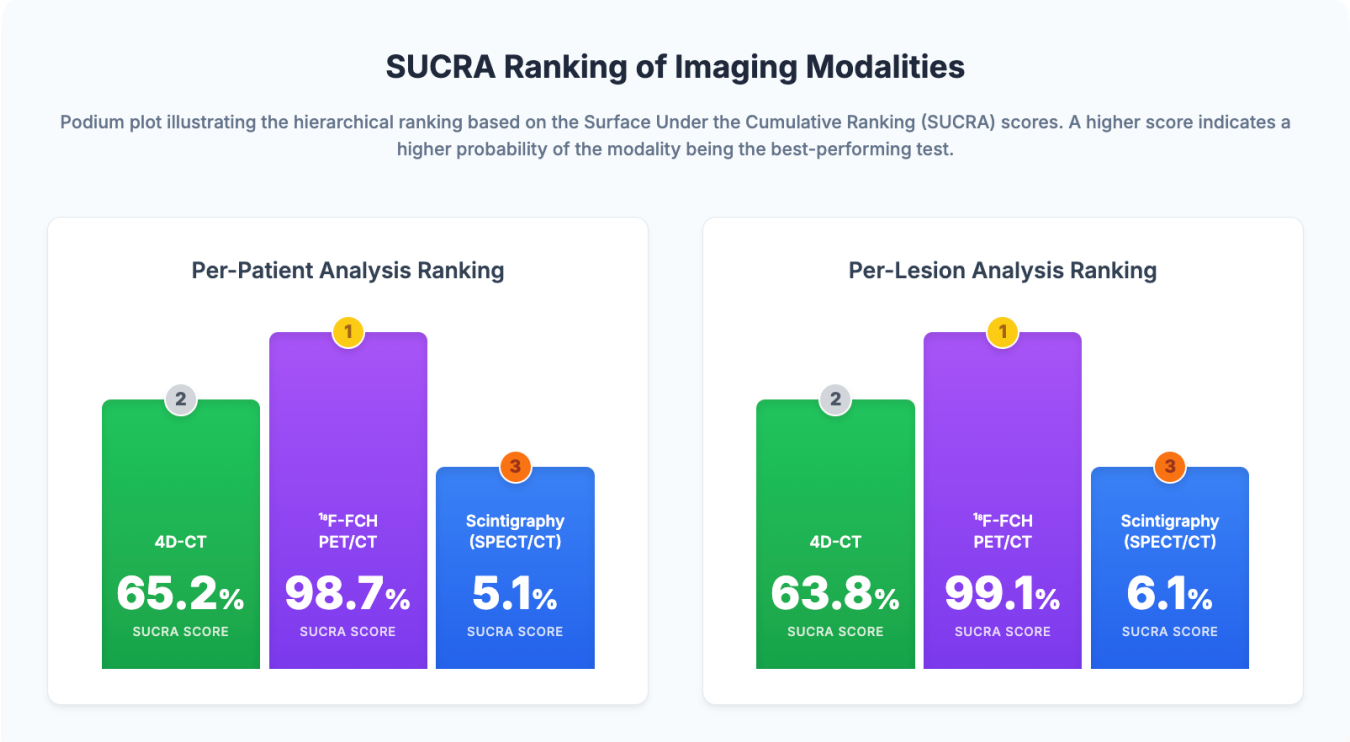

Figure 5. SUCRA ranking of imaging modalities.

The biological target of ^{18}F-FCH is the enzyme choline kinase A (CHKA), which catalyzes the rate-limiting step in the synthesis of phosphatidylcholine, an essential component of cell membranes.[12] In tissues characterized by high rates of cellular proliferation and membrane turnover—a defining feature of hyperfunctioning parathyroid adenomas and hyperplastic glands—the expression and activity of CHKA are dramatically upregulated. This upregulation creates a powerful "metabolic trap" for the radiolabeled choline analog, ^{18}F-FCH, leading to its intense accumulation within the culprit parathyroid tissue. The true elegance of this mechanism is revealed in the context of the reoperative neck.[13] A prior surgery transforms the neck into an anatomical minefield of scar tissue, fibrosis, inflammation, and disrupted vascular pathways. These changes are precisely the factors that confound imaging modalities reliant on anatomical clarity or predictable perfusion. ^{18}F-FCH PET/CT, however, effectively bypasses these challenges. Its signal is generated at a cellular and molecular level, contingent only on the biological state of the parathyroid tissue itself. A small, 4mm adenoma, encased in dense scar tissue and adherent to the recurrent laryngeal nerve—a scenario that would render it invisible to ultrasound and anatomically ambiguous on CT—will still shine brightly on an ^{18}F-FCH PET scan as long as it is overexpressing CHKA. This explains its unparalleled ability to detect small, ectopic, and deeply seated lesions that are the common causes of surgical failure. The resulting high target-to-background ratio provides a clear, unambiguous signal, empowering the clinician with a high degree of diagnostic confidence and providing the surgeon with a precise target for a focused re-exploration.[14]

Our analysis positions 4D-CT as a capable second-tier modality, significantly outperforming scintigraphy but falling short of ^{18}F-FCH PET/CT. Its strength lies in its exquisite spatial resolution and its ability to

characterize the unique hemodynamic signature of parathyroid adenomas: avid arterial enhancement and rapid venous washout. In an unoperated neck, this technique is formidable. However, the reoperative field systematically degrades the very parameters that 4D-CT relies upon. Firstly, the primary arterial supply to a missed gland, often a branch of the inferior thyroid artery, may have been ligated or compromised during the initial operation. This can fundamentally alter the gland's enhancement dynamics, blunting the arterial "flash" and making its signature less distinct. Secondly, post-surgical fibrosis and granulation tissue are major confounders. This reactive tissue is often hyperemic and can enhance avidly, creating false-positive findings that can be mistaken for a true adenoma. A reactive lymph node, a common finding after neck surgery, presents a classic diagnostic dilemma on 4D-CT. Thirdly, the obliteration of natural fat planes by scarring makes morphological assessment challenging.[15] A small adenoma may become inseparable from adjacent structures like the trachea or esophagus. The 12-point gap in per-patient sensitivity between ^{18}F-FCH PET/CT and 4D-CT in our analysis likely represents this cohort of patients, where the anatomical and perfusion-based diagnosis of 4D-CT was defeated by the consequences of the prior surgery.

The finding that modern ^{99m}Tc-Sestamibi SPECT/CT achieved a per-patient sensitivity of only 60% confirms its significant limitations in this context. This is not a failure of technology—SPECT/CT provides excellent anatomical fusion—but rather a failure of the underlying biology of the radiopharmaceutical. Sestamibi uptake is contingent on two key factors: adequate blood flow for delivery and high mitochondrial density for retention. Both can be compromised in the reoperative patient. Perfusion can be diminished, as discussed for 4D-CT, leading to poor tracer delivery. More fundamentally, the biological variability of parathyroid adenomas is a major hurdle. Not all adenomas are rich in mitochondria; those that are predominantly composed of chief cells may have insufficient mitochondrial density for avid sestamibi retention.[16] Furthermore, the expression of the P-glycoprotein (MDR1) efflux pump is a critical variable. High P-gp expression will actively pump sestamibi out of the cell, leading to rapid washout and a false-negative scan. These biological factors, combined with the inherently lower spatial resolution of scintigraphy compared to PET or CT, render it an unreliable tool for the high-stakes task of guiding reoperative surgery.[17]

The hierarchical evidence from this NMA demands a re-evaluation of current clinical practice. The traditional, often sequential, imaging approach is inefficient and, as our data show, suboptimal.[18] Based on this analysis, we propose a new, evidence-based algorithm that also considers real-world constraints of cost and accessibility. In a patient with biochemically confirmed persistent/recurrent PHPT, the unequivocal first-line imaging modality should be ^{18}F-FCH PET/CT.[19] Its superior per-patient and per-lesion sensitivity maximizes the likelihood of successful localization in a single step, enabling a confident, focused reoperation. This approach is likely the most cost-effective in the long term, as the high upfront cost of the scan is offset by the avoidance of further negative imaging studies, reduced operative time, and, most critically, the prevention of a third, even more complex and costly, operation.[20] We recognize that ^{18}F-FCH PET/CT is not universally available. Therefore, a pragmatic, tiered algorithm is necessary: Tier 1 Centers (with PET/CT access): Implement the ideal pathway, using ^{18}F-FCH PET/CT as the first-line test; Tier 2 Centers (without PET/CT access): The first-line modality should be high-quality 4D-CT. Given its 82.5% sensitivity, it remains a powerful tool. However, if the 4D-CT is negative or equivocal, there should be a low threshold for referral to a Tier 1 center for ^{18}F-FCH PET/CT rather than proceeding to a potentially futile exploratory surgery; The Role of Scintigraphy: ^{99m}Tc-Sestamibi SPECT/CT should be de-emphasized as a primary localization tool in this setting. Its use should be reserved for problem-solving in rare cases or in settings where neither PET/CT nor high-quality 4D-CT is available. This tiered approach balances the

pursuit of the best possible diagnostic accuracy with the practical realities of healthcare systems worldwide. It is also critical to consider the radiation burden of these investigations (Figure 6). While ^{18}F-FCH PET/CT and 4D-CT provide the highest accuracy, they also impart the highest radiation dose, a factor that should be considered in clinical decision-making, particularly in younger patients.

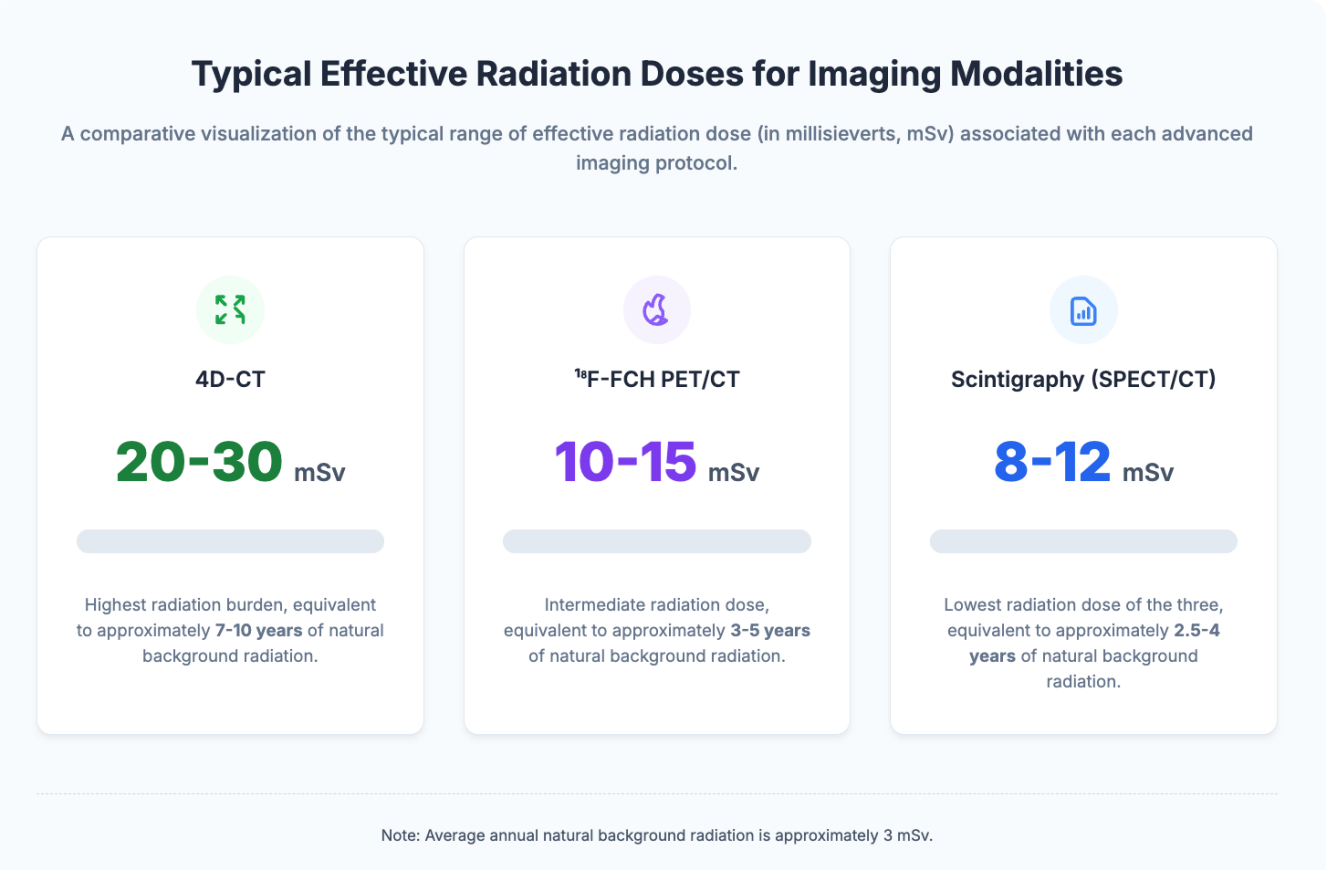

Figure 6. Typical effective radiation doses for imaging modalities.

Figure 7 showed a detailed schematic infographic that masterfully illustrates the pathophysiological basis for the hierarchical imaging performance observed in the reoperative neck. By dissecting the distinct biological mechanisms each modality relies on, the figure provides a clear, scientific rationale for why ^{18}F-FCH PET/CT demonstrates superior performance, why 4D-CT faces anatomical challenges, and why scintigraphy is hampered by biological hurdles. This visual narrative is essential for understanding not just that one test is better, but why it is fundamentally more suited to this complex clinical scenario. The first panel of the figure, dedicated to ^{18}F-FCH PET/CT, immediately establishes its superior standing. The schematic diagram is particularly insightful; it depicts a parathyroid cell situated within a background representing a scarred, surgically altered field. Critically, the radiotracer, ^{18}F-FCH, is shown entering the cell and undergoing "Metabolic Trapping." This process is driven by the overexpression of Choline Kinase A (CKA), an enzyme integral to cell membrane synthesis. In hyperfunctioning, proliferative parathyroid tissue, the demand for new cell membranes is high, leading to a significant upregulation of CKA. This enzyme phosphorylates the ^{18}F-FCH upon entry, trapping it

within the cell and causing a high concentration of the positron-emitting tracer. The key takeaways below the schematic reinforce this concept. The modality's success is rooted in Metabolic Targeting, a mechanism that interrogates the intrinsic biological activity of the culprit gland. This is a profound advantage because, as the second point highlights, its performance is Immune to Anatomy. The fibrotic tissue, inflammation, and disrupted blood vessels that characterize a reoperative neck—and confound other imaging techniques—are essentially invisible to this metabolic signal. The PET scanner detects the intense focal accumulation of the tracer irrespective of the surrounding anatomical chaos. This results in an exceptionally high signal-to-background ratio, where the hyperfunctioning gland appears as a bright, unmistakable beacon, providing the surgeon with a clear and confident target. The central panel, focusing on 4D-CT, accurately portrays it as a powerful but flawed modality in this setting. The schematic shows a parathyroid gland and a nearby lymph node (LN), both receiving contrast flow. This visual immediately hints at the primary challenge of this technique: differentiating the target tissue from its mimics. The first explanatory point, Perfusion & Anatomy, speaks to the strengths of 4D-CT. Its excellent spatial resolution allows for precise anatomical delineation, and its multi-phasic nature is designed to capture the unique vascular signature of an adenoma—avid arterial enhancement and rapid washout. In a pristine, unoperated neck, this combination is highly effective. However, the second point, Confounded by Scarring, reveals its Achilles' heel in the reoperative patient. The scarred environment creates two major problems. First, fibrosis can physically obscure the anatomical planes, making a small adenoma difficult to distinguish from the surrounding tissue. More importantly, scarring alters the very blood flow that 4D-CT relies on for diagnosis. A compromised artery may lead to a blunted or atypical enhancement pattern in the true adenoma, causing a false negative. Conversely, post-surgical inflammation can make other structures, such as reactive lymph nodes, hyperemic. These nodes can enhance avidly with contrast, perfectly mimicking the appearance of a parathyroid adenoma and leading to a false-positive result. Therefore, while 4D-CT provides a beautiful anatomical map, the landmarks on that map can be misleading in a post-surgical landscape. The final panel illustrates why scintigraphy, even with modern SPECT/CT, struggles in this context. The schematic of the parathyroid cell is brilliantly informative, showing the ^{99m}Tc-MIBI tracer entering but also being actively ejected by an efflux pump (P-gp). This visual encapsulates the two fundamental biological weaknesses of the technique. The first hurdle is its Mitochondrial Dependence. The uptake and retention of ^{99m}Tc-MIBI are contingent on high mitochondrial density within the parathyroid cells. However, this is not a uniform feature of all adenomas. Those that are "mitochondria-poor," often composed primarily of chief cells rather than oxyphil cells, will not accumulate the tracer avidly, regardless of their hormonal activity. This inherent biological variability means the test is destined to fail in a significant subset of patients from the outset. The second, and perhaps more insidious, hurdle is P-glycoprotein (P-gp) Efflux. P-gp is a transmembrane pump that actively expels various substances from the cell, including ^{99m}Tc-MIBI. If a parathyroid adenoma overexpresses this pump, the tracer may be efficiently ejected from the cell almost as quickly as it enters. This leads to rapid washout, erasing the signal difference between the parathyroid and surrounding tissue that is necessary for detection. This phenomenon can cause a false-negative scan even in a mitochondria-rich adenoma with good initial blood flow. These two biological hurdles, combined with the inherently lower spatial resolution of scintigraphy, create a perfect storm of limitations that severely compromise its reliability for guiding high-stakes reoperative surgery.

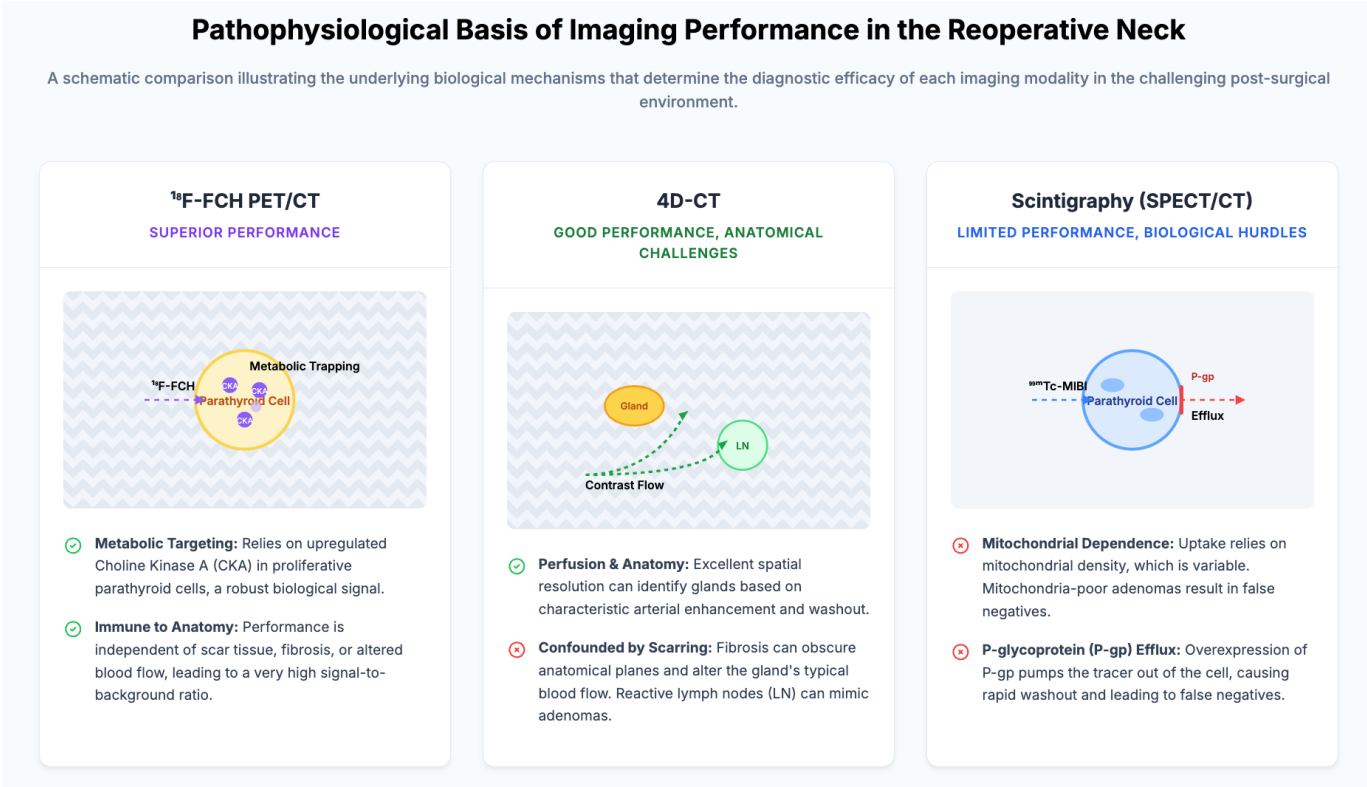

Figure 7. Pathophysiological basis of imaging performance in the reoperative neck.

5. Conclusion

This network meta-analysis provides definitive, high-level evidence that ^{18}F-FCH PET/CT offers superior diagnostic performance for the localization of hyperfunctioning parathyroid tissue in the challenging setting of persistent or recurrent primary hyperparathyroidism. Its accuracy, rooted in robust metabolic targeting that transcends the anatomical and physiological disruptions of prior surgery, establishes it as the premier imaging modality. These findings strongly support a paradigm shift in clinical practice, advocating for the adoption of diagnostic algorithms that prioritize ^{18}F-FCH PET/CT. By doing so, we can enhance the precision of surgical planning, increase the success rates of reoperative parathyroidectomy, minimize patient morbidity, and set a new standard of care for this complex endocrine disease.

6. References

1. Latge A, Riehm S, Vix M, Bani J, Ignat M, Pretet V, et al. ^{18}F-fluorocholine PET and 4D-CT in patients with persistent and recurrent primary hyperparathyroidism. Diagnostics (Basel). 2021; 11(12): 2384.
2. Yanar C, Kostek M, Unlu MT, Caliskan O, Dincer B, Cetinoglu I, et al. The role of 4D-CT for pre-operative localization in patients with primary hyperparathyroidism with negative ultrasonography and/or sestamibi SPECT/CT. SiSli Etfal Hastan Tip Bul / Med Bull Sisli Hosp. 2023; 57(2): 238–44.
3. Barranquero AG, Pastor P, Ortega A, Corral S, Gómez Ramírez J, Luengo P, et al. 4D-CT as a second line preoperative localization test for the evaluation of primary hyperparathyroidism. Cir Esp (Engl Ed). 2023; 101(8): 530–7.

4. Xiao J, Wang D. Hyperparathyroidism caused by intrathyroidal parathyroid adenoma detected by ^{99m}Tc-sestamibi parathyroid scan and ^{18}F-fluorocholine PET/CT. Jpn J Clin Oncol. 2022; 52(4): 397–8.
5. Dudoignon D, Delbot T, Cottereau AS, Dechmi A, Bienvenu M, Koumakis E, et al. ^{18}F-fluorocholine PET/CT and conventional imaging in primary hyperparathyroidism. Diagn Interv Imaging. 2022; 103(5): 258–65.
6. Messaoud L, Amiot H-M, Lecuru F, Cottu PH, Cassou-Mounat T. Discovery of peritoneal carcinomatosis on ^{18}F-fluorocholine PET/CT performed for primary hyperparathyroidism. Rev Esp Med Nucl Imagen Mol (Engl Ed). 2023; 42(1): 38–9.
7. Imperiale A, Bani J, Bottoni G, Latgé A, Heimburger C, Catrambone U, et al. Does ^{18}F-fluorocholine PET/CT add value to positive parathyroid scintigraphy in the presurgical assessment of primary hyperparathyroidism? Front Med (Lausanne). 2023; 10: 1148287.
8. Rizzo A, Racca M, Cauda S, Balma M, Dall'Armellina S, Dionisi B, et al. ^{18}F-fluorocholine PET/CT semi-quantitative analysis in patients affected by primary hyperparathyroidism: a comparison between laboratory and functional data. Endocrine. 2023; 80(2): 433–40.
9. Te Beek ET, van Duijnhoven CPW, Slart RHJA, van den Bergh JP, Ten Broek MRJ. Quantitative CT evaluation of bone mineral density in the thoracic spine on ^{18}F-fluorocholine PET/CT imaging in patients with primary hyperparathyroidism. J Clin Densitom. 2024; 27(1): 101464.
10. Kesim S, Turoglu HT, Kotan T, Balaban Genc ZC, Niftaliyeva K, Toper H, et al. Efficacy of additional lateral pinhole and SPECT/CT imaging in dual-phase Tc-99m MIBI parathyroid scintigraphy for localising parathyroid pathologies in patients with primary hyperparathyroidism: a single-institution experience. Nucl Med Commun. 2025; 46(1): 47–54.
11. Pasini Nemir E, Fares S, Rogić I, Golubić AT, Huić D. ^{18}F-fluorocholine PET/CT imaging in primary hyperparathyroidism after negative or inconclusive cervical ultrasonography and ^{99m}Tc-MIBI scintigraphy. Jpn J Radiol. 2025; 43(4): 687–95.
12. Siordia Cruz NS, Gallegos De Luna CF, Ramírez-Preciado II, Zavala Mejía JJ, Peña Montañez GA, González MS, et al. Comparison of ultrasonography and scintigraphy as localization techniques in the preoperative evaluation of primary hyperparathyroidism. Cureus. 2025; 17(4): e82021.
13. Jitrapinate W, Raruenrom Y, Wongsurawat N, Sa-Ngiamwibool P, Theerakulpisut D. SPECT/CT in addition to subtraction parathyroid scintigraphy in hyperparathyroidism: diagnostic performance in a cohort of predominantly end-stage renal disease patients. EJNMMI Res. 2025; 15(1): 34.
14. Loryś L, Klimczak K, Budzyńska K, Narloch M, Kasprzak S, Kasprzak K, et al. Comparison of first- and second-line imaging diagnostics (ultrasound + scintigraphy and PET + 4DCT) in visualizing parathyroid glands in primary hyperparathyroidism including ectopic foci. J Educ Health Sport. 2025; 82: 60366.
15. Park Y-J, Kim SJ, Choi D, Hyun SH. Artificial delayed-phase technetium-99m MIBI scintigraphy from early-phase scintigraphy improves identification of hyperfunctioning parathyroid lesions in patients with hyperparathyroidism. Clin Nucl Med. 2025; 50(7): 631–8.
16. Mi J, Fang Y, Xian J, Wang G, Guo Y, Hong H, et al. Comparative effectiveness of MRI, 4D-CT and ultrasonography in patients with secondary hyperparathyroidism. Ther Clin Risk Manag. 2023; 19: 369–81.

17. Keven A, Gürbüz AF, Arslan G. The role of 4D-CT in hyperparathyroidism with negative scintigraphy: Identifying causes of diagnostic challenges. Bezmialem Sci. 2025; 13(2): 139–47.
18. Bouilloux E, Santucci N, Bertaut A, Alberini J-L, Cochet A, Drouet C. Diagnostic performances of ^{18}F-fluorocholine PET/CT as first-line functional imaging method for localization of hyperfunctioning parathyroid tissue in primary hyperparathyroidism. Acad Radiol. 2025; 32(2): 743–53.
19. Chiu W-Y, Chen K-Y, Shun C-T, Wu M-H, Tsai K-S, Chiu C-H, et al. Conventional imaging techniques plus ^{18}F-fluorocholine PET/CT: a comparative study of diagnostic accuracy in localizing parathyroid adenomas in primary hyperparathyroidism. Front Endocrinol (Lausanne). 2025; 16(1595461): 1595461.
20. Wootton E, Wong C, Love A, Pattison DA. Successful localization of recurrent MEN-1-associated hyperparathyroidism with ^{18}F-fluorocholine PET/CT. JCEM Case Rep. 2024; 2(12): luae222.